

Seven-coordinated Silicon in a SiO_2He Compound Formed under the Extreme Conditions of Planetary Interiors

Shicong Ding,¹ Pan Zhang,¹ Kang Yang,¹ Cailong Liu,² Jian Hao,¹ Wenwen Cui,^{1,*} Jingming Shi,^{1,†} and Yinwei Li^{1,2,‡}

¹*Laboratory of Quantum Materials Design and Application, School of Physics and Electronic Engineering, Jiangsu Normal University, Xuzhou 221116, China*

²*Shandong Key Laboratory of Optical Communication Science and Technology, School of Physical Science & Information Technology of Liaocheng University, Liaocheng 252059, China*

(Dated: November 7, 2021)

Changes in atomic coordination numbers at high pressures are fundamental to condensed-matter physics because they initiate the emergence of unexpected structures and phenomena. Silicon is capable of forming eight-, nine-, and ten-coordinated structures under compression, in addition to the usual six-coordinated structures. The missing seven-coordinated silicon remains an open question, but here our theoretical study provides evidence for its existence at high pressures. A combination of a crystal-structure prediction method and first-principles calculations allowed prediction of a stable SiO_2He compound containing unique SiO_7 polyhedrons, which is a configuration unknown in any proposed silica phase. Consequently, seven-coordinated SiO_7 is a possible form of silica at high pressures. Further calculations indicate that the SiO_2He phase remains energetically stable with a solid character over a wide range of pressures exceeding 607 GPa and temperatures of 0–9000 K, covering the extreme conditions of the core–mantle boundary in super-Earth exoplanets, or even the Solar System’s ice giant planets. Our results may provide theoretical guidance for the discovery of other silicides at high pressures, promote the exploration of materials at planetary core–mantle boundaries, and enable planetary models to be refined.

Silica (SiO_2) is the main component of silicates in the core–mantle boundary (CMB) of the Earth and super-Earth exoplanets (1–10 times Earth’s mass, M_\oplus). It has therefore attracted much recent attention in the fields of condensed matter physics, high-pressure physics, and planetary sciences [1–3]. Elucidating the high-pressure behavior of silica (like existence, form, and phase transition) is crucial for modeling the structure, formation, and evolution of planets. At ambient conditions, quartz is the most common stable phase of SiO_2 [4]. Compressing SiO_2 induces a complicated series of phase transitions; i.e., quartz phase \rightarrow coesite phase (~ 2 GPa) [5] \rightarrow stishovite phase (~ 10 GPa) [6, 7] \rightarrow CaCl_2 -type phase (~ 48 GPa) [8] \rightarrow α - PbO_2 -type (~ 82 GPa) [9, 10] \rightarrow pyrite-type phase (~ 260 GPa) [11, 12]. These crystalline SiO_2 phases such as CaCl_2 -, α - PbO_2 -, and pyrite-type have a same Si coordination number of six while for the glassy state of SiO_2 may structurally evolve above 95 GPa to have a Si coordination number greater than six [13] which is proposed by experiment. Recent work has predicted a silica $R\bar{3}$ phase with mixed six-, eight-, and nine-fold coordination stabilized at 645 GPa, which subsequently transforms into the Fe_2P -type structure at 890 GPa [14]. With respect to temperature, the cotunnite-type phase is much more stable than the $R\bar{3}$ or Fe_2P -type phases of SiO_2 [1, 2, 15]. Coordination in the cotunnite- and Fe_2P -type phases can reach nine under extremely high pressure and temperature. Finally, the Fe_2P -type structure transforms into the $I4/mmm$ phase with a coordination number of 10 at 10 TPa [16].

Planetary interiors are naturally extremely hot, pressurized, and rich in silica. Understanding the silica structure before it melted under extreme conditions is the key to determining a planet’s internal structure and evolution. In 2015, Millot *et al.*’s laser-driven shock experiment found that the melting temperature of silica rises to 8300 K at a pressure of 500 GPa, comparable to the CMB of a super-Earth of $5M_\oplus$ [3]. However, laboratory experiments face several challenges when reproducing the conditions of giant planets or super-Earths [17]. Theoretical modeling can effectively simulate extreme conditions and so aid exploration of the behavior of minerals such as SiO_2 inside planetary interiors [2, 15, 18–20]. Using first-principles molecular dynamics simulations, Scipionia *et al.* found that under conditions of the early Earth’s and super-Earths’ deep molten mantles, the electron conductivity of liquid SiO_2 was sufficiently large to support a silicate dynamo. [18]. Felipe *et al.* studied the melting curves of SiO_2 up to 6 TPa using first-principles molecular dynamics simulations, finding that SiO_2 is solid under the conditions of the cores of all the solar system’s gas giants and also super-Earths of $10 M_\oplus$ [19]. Taku *et al.* and Wu *et al.* independently proposed that the cores of Uranus and Neptune are expected to consist of Fe_2P -type silica and MgSiO_3 [2, 15]. Niu *et al.*’s structural prediction of the Mg–Si–O ternary phase diagram under exoplanet pressure revealed two novel compounds, Mg_2SiO_4 and MgSi_2O_5 , as being stable at the CMB of large super-Earths [20]. Overall, these studies make important contributions to the understanding of the physicochemical diversity of planetary systems.

Helium is the second most abundant element in the universe, and is extensively present in stars and gas giant planets [21, 22]. It is usually chemically inert and does not react easily with other substances at ambient conditions due to its

* wenwencui@jsnu.edu.cn

† jingmingshi@jsnu.edu.cn

‡ yinwei.li@jsnu.edu.cn

closed-shell electronic configuration. The melting and volcanic effects of the early Earth's mantle caused He in the upper mantle to escape via internal degassing and disappear into space, while a layer of the lower mantle continues to retain He [23]. Recent studies have shown that FeO_2 can react with He near the Earth's CMB to trap He in the lower mantle [24]. Ice giants are mainly composed of H_2O , NH_3 , and CH_4 ; their atmospheres are rich in He [21, 25]. Theoretical studies have shown that H_2O [26–28], NH_3 [28–30], and CH_4 [31] can form stable compounds with He at high pressure, and first-principles molecular dynamics suggests that both H_2O –He and NH_3 –He may exist in a superionic state in the interiors of icy planets, in addition to the plastic state of NH_3 –He and the plastic or partially diffusive state of CH_4 –He at lower pressures and temperatures. Theoretical study reported that He can form stable crystalline compounds with iron at terapascal pressures [32]. Other recent studies have reported the high-pressure stability of He–alkali oxides (sulfides) [33], HeN_4 [34], Na_2He [35], $\text{Mg}(\text{Ca})\text{F}_2\text{He}$ [36], and XeHe_2 [37].

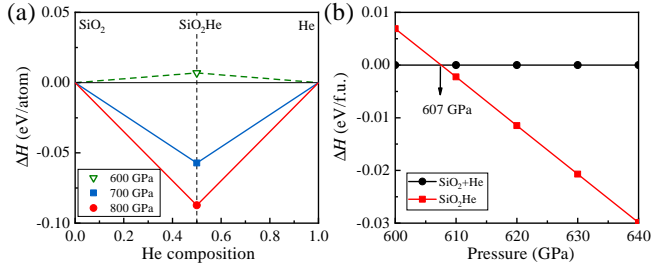


FIG. 1. (a) Convex hull for formation enthalpies (ΔH) of the SiO_2 –He system at selected pressures, defined as $\Delta H = [H((\text{SiO}_2)_x\text{He}_y) - xH(\text{SiO}_2) - yH(\text{He})] / (3x + y)$. (b) Calculated formation enthalpy of SiO_2He relative to decomposition products SiO_2 (pyrite-type at 600 GPa, $R\bar{3}$ at 700 and 800 GPa) and He (*hcp* at 600–800 GPa) as a function of pressure.

Previous studies have shown that the insertion of He into cristobalite can greatly decrease its compressibility, resulting in two cristobalite–helium compound phases; i.e., I ($P2_1/c$, stable above 6.4 GPa) and II ($R\bar{3}c$, at 1.7–6.4 GPa) [38, 39]. Despite substantial experimental and theoretical efforts to understand the compositions of planetary interiors, the results are far from sufficient. The nature of SiO_2 under extreme conditions, especially in combination with other elements, in planetary interiors requires further investigation; its elucidation would greatly aid our understanding of planetary formation and evolution.

Combining density function theory and structural prediction, this work performs an extensive exploration of the SiO_2 –He systems at high pressure and high temperature. The results show that He can react with SiO_2 to form $Pnma$ SiO_2He at high pressures, and first-principles molecular dynamics simulations indicate that solid $Pnma$ SiO_2He exists in the mantle of Uranus and Neptune, as well as the CMB of Saturn and super-Earth exoplanets. Interestingly, $Pnma$ SiO_2He has four equivalent seven-coordinated SiO_7 octahedra. Previ-

ously, only six-, eight-, nine-, and 10-coordination has been reported in the stable high-pressure phases of SiO_2 , with seven-coordinated SiO_2 as a metastable phase [2, 14]. Our study suggests that seven-coordinated SiO_7 might be present in $Pnma$ SiO_2He at high pressure.

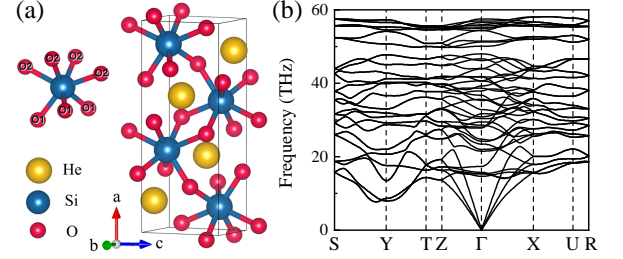


FIG. 2. (a) Crystal structure predicted for $Pnma$ SiO_2He at 700 GPa and the equivalent SiO_7 octahedron. Yellow, blue, and red spheres represent He, Si, and O atoms, respectively. (b) Calculated phonon dispersions of $Pnma$ SiO_2He at 700 GPa.

Structure predictions for the SiO_2 –He system are performed here using CALYPSO [40, 41], based on a global minimization of free energy surfaces in conjunction with *ab initio* total-energy calculations, which has been used successfully to predict various systems under high pressure [42–45]. Structural relaxations are performed using density functional theory as implemented in the Vienna *ab initio* simulation package [46, 47], adopting the Perdew–Burke–Ernzerhof exchange–correlation functional under the generalized gradient approximation [48, 49]. All-electron projector augmented wave pseudopotentials with $3s^23p^2$, $2s^22p^4$, and $1s^2$ valence configurations are chosen for Si, O, and He atoms, respectively [50]. Structure searches use a plane wave cutoff energy of 1000 eV and k-point mesh of $2\pi \times 0.04 \text{ \AA}^{-1}$. The lowest-energy structural optimization and electronic properties are calculated using ‘hard’ pseudopotentials with $2s^22p^63s^23p^2$ and $2s^22p^4$ valence configurations for Si and O atoms, respectively. A plane wave cutoff energy of 1500 eV and k-point mesh of $2\pi \times 0.03 \text{ \AA}^{-1}$ are set to ensure total energy and forces convergence better than 1 meV/atom and 1 meV/Å, respectively. Phonon calculations are carried out using a supercell approach, as implemented in PHONOPY code [51]. *Ab initio* molecular dynamics (AIMD) simulations [52] explore the form of SiO_2He compounds at high pressures and high temperatures. A $2 \times 2 \times 2$ supercell of 288 atoms is employed, along with Γ point sampling of the Brillouin zone. The canonical NVT (N -number of particles, V -volume, and T -temperature) ensemble uses a Nose–Hoover thermostat [53] with $\text{SMASS} = 2$, and each simulation consists of 20,000 time steps of 0.5 fs. We allow 1 ps for thermalization, and then exact data for 4 ps. The crystal structures and electron localization function (ELF) are plotted using VESTA software [54].

Extensive structure searches for $(\text{SiO}_2)_x\text{He}_y$ ($x, y = 1–3$) are performed at 100–800 GPa with maximum simulation cells up to four formula units (f.u.) at each composition.

Fig. 1(a) summarizes the formation enthalpies (ΔH) of the stoichiometries with respect to decomposition into SiO_2 and He, with positive formation enthalpies above 0.05 eV/atom not shown in the convex hull. The stoichiometry of SiO_2He is identified with a negative formation enthalpy at 700 and 800 GPa, whose ΔH approaches zero at ~ 607 GPa, as shown in Fig. 1(b). This reveals that the SiO_2He compound is thermodynamically stable when the pressure is above the critical pressure.

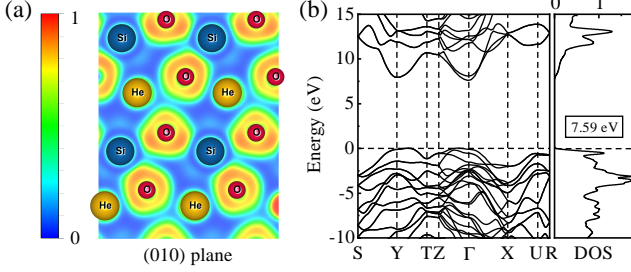


FIG. 3. (a) ELF and (b) electronic band structures (left) and density of states (DOS; right) of $Pnma$ SiO_2He at 610 GPa.

The predicted SiO_2He phase has an orthorhombic structure with space group $Pnma$ (4 f.u. in a unit cell) and remains stable up to 1000 GPa, the maximum pressure studied here. Fig. 2(a) shows the structural configuration of $Pnma$ SiO_2He , and Table S1 in the Supplemental Material summarizes the detailed structural parameters [55]. By further analysis of the atomic positions, we find that all the silicon atoms in our predicted $Pnma$ SiO_2He phase are with seven coordination. Each Si atom and its seven surrounding O atoms form a SiO_7 polyhedron, which is never reported by previous studies in Si-O systems and reveals the emergence of a novel mode of bonding for Si-O under high pressure. Four SiO_7 polyhedra in the unit cell are equivalent with Si-O bond lengths ranging from 1.54 to 1.67 Å. Two SiO_7 polyhedra in the center of the cell connect with each other by sharing edges and connect to the top and bottom sides by sharing vertices. There are two kinds of O atom, which are located in the $4c$ Wyckoff positions. Surprisingly, the He atoms occupy positions similar to Si atoms in the SiO_7 polyhedra. If considering only the relative positions of He and O atoms, they can also form a HeO_7 polyhedral structure nearly identical to the SiO_7 polyhedra with He-O distances ranging from 1.51 to 1.71 Å. The volumes of the polyhedra are 5.85 Å^3 for HeO_7 and 5.79 Å^3 for SiO_7 (see Figure S1 in the Supplemental Material [55]). If we take the $Pnma$ SiO_2He phase as prototype structure and choose Si atoms to substitute all the He atoms, we can obtain a novel SiO compounds with the same $Pnma$ symmetry. Unfortunately, calculation results show that the formation enthalpy of this new SiO compound is about 0.71 eV/atom with respect to SiO_2 and Si, while about -0.76 eV/atom with respect to elements at 700 GPa, which reveals that the designed structure might be a metastable phase of Si-O compound. If this phase can be synthesized on experiment, which reveals

that a novel unconventional silicon coordination Si-O compound is exist under high pressure. Phonon calculations reveal that there are no imaginary dispersions of $Pnma$ SiO_2He at 700 (Fig. 2(b)), 610, or 800 GPa (Supplemental Material Figure S2 [55] for both), confirming the robust dynamic stability of $Pnma$ SiO_2He .

Fig. 3(a) shows the ELF of $Pnma$ SiO_2He to analyze the bonding features of He inserted in SiO_2 . The electrons are strongly localized in O atoms and delocalized around Si, indicating ionic bonding between these atoms, which is consistent with our Bader charge analysis calculation results [56]. The Bader charge transfer calculations for the SiO_2He structure at 610 GPa show that a Si atom loses $\sim 3.39 e^-$, $1.64 e^-$ of which is transferred to oxygen atom O_1 , $1.67 e^-$ to oxygen atom O_2 , and only $\sim 0.08 e^-$ to He. The near complete absence of charge transfer between SiO_2 and He indicates that He atoms do not chemically bond with neighboring atoms. Other He-containing systems behave similarly: for example, FeO_2He [24], $\text{H}_2\text{O-He}$ [26–28], $\text{NH}_3\text{-He}$ [28–30], HeN_4 [34], and Na_2He [35]. Electronic band structure and DOS calculations show that $Pnma$ SiO_2He is an insulator with a band gap of 7.59 eV at 610 GPa (Fig. 3(b)). Further compression slightly increases the band gap to 8.26 eV at 1 TPa (cf. Figure S3 in the Supplemental Material [55]).

The interiors of planets harbor conditions of high pressure and high temperature. In order to determine the stable regions of pressure and temperature for $Pnma$ SiO_2He , we consider the temperature effect using the harmonic approximation by performing the phonon dispersion calculations for all the structures in 600, 700, 800, 900 and 1000 GPa. We calculate the formation energy of $Pnma$ SiO_2He with respect to the decomposition products SiO_2 and He under high pressure and temperature. The critical boundary of stability (white line) is plotted in the phase diagram of the SiO_2 system, as shown in Fig. 4(a). For example, our calculations show that the $Pnma$ SiO_2He phase is stable at 800 GPa when the temperature is below 7000 K, above that it will decompose into SiO_2 and He. AIMD simulations consider the form of $Pnma$ SiO_2He at the conditions of giant planets; i.e., pressures of 600–1000 GPa and temperatures of 0–10,000 K. Fig. 4(b) shows the calculated mean squared displacement (MSD) of atomic positions and atoms trajectories for Si (blue), O (red), and He (orange). At $P = 800$ GPa and $T = 7000$ K, all atoms in SiO_2He vibrate around their lattice positions and the diffusion coefficients are zero ($D^{\text{Si}} = D^{\text{O}} = D^{\text{He}} = 0$), indicating that the $Pnma$ SiO_2He phase remains solid at these conditions. Fig. 4(a) can clearly depict its form inside gas giants and super-Earths. The yellow gradient area in the figure indicates $Pnma$ SiO_2He as being a stable solid. As the super-Earths' mantle adiabat crosses the region of stable $Pnma$ SiO_2He , $Pnma$ SiO_2He may be present within the CMBs of super-Earths larger than $5.7 M_{\oplus}$. Potential examples include exoplanets Kepler-99 b, Kepler-406 b, LHS 1140 b, Kepler-18 b, and Kepler-100 b (purple crosses in the figure). Figure S4 in the Supplemental Material [55] shows mass-radius relations for these Earth-like structures. Recent studies have

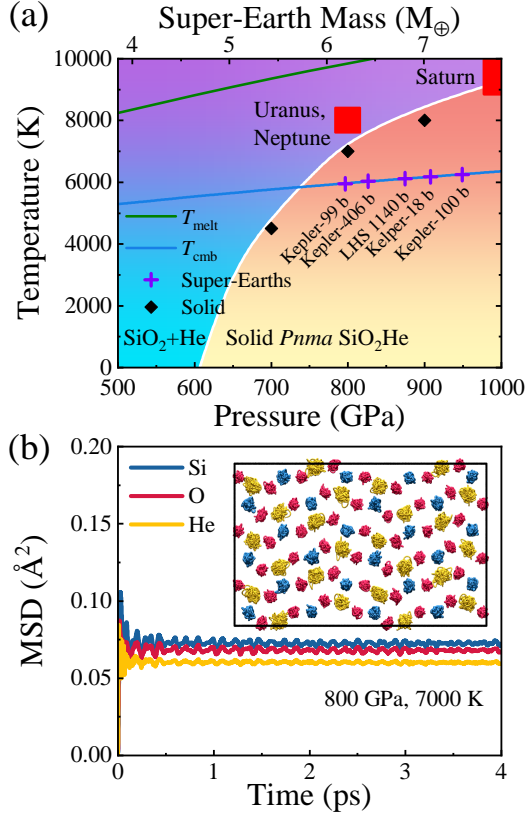


FIG. 4. (a) Pressure-temperature (P - T) phase diagram showing the stability field of $Pnma$ SiO_2He and its boundary (white line) with the decomposition products $\text{SiO}_2 + \text{He}$. Black diamonds represent solid $Pnma$ SiO_2He . Red squares indicate the CMB of Uranus, Neptune, and Saturn [57]. The proposed silica melting line ($T_m = 1968.5 + 307.8 P_m^{0.485}$) [3] and the super-Earths' mantle adiabat ($T_{cmb} = 2275.2 + 1583.5 \left(\frac{P}{129.8}\right)^{0.485}$) [58] are plotted in green and blue, respectively. $P = 129.8 \left(\frac{M_S}{M_E}\right)$ links the pressure scale to the super-Earth mass (M_S) scale [58]. Purple crosses indicate some Earth-like super-Earths with pressure corresponding to that in T_{cmb} . (b) Calculated mean squared displacement (MSD) of the atomic positions of $Pnma$ SiO_2He at 800 GPa and 7000 K. Insert gives atomic trajectories in one supercell from the simulations in the last 2 ps.

indicated an unclear distinction between the mantle and the core of Uranus and Neptune [59]; the CMB of both is slightly above the region of $Pnma$ SiO_2He , suggesting that $Pnma$ SiO_2He may be present in both planets' mantles. Saturn is a gas giant with much He in its mantle. Some of its CBM overlaps with the stable region of $Pnma$ SiO_2He , suggesting that $Pnma$ SiO_2He may also be present in Saturn's CBM. We also calculate the MSD of $Pnma$ SiO_2He at high temperatures to study each atom's behavior, as shown in Fig. S5 and Fig. S6. The calculations show that $P = 700$ GPa, $T = 4500$ K and $P = 900$ GPa, $T = 8000$ K can be viewed as critical conditions of $Pnma$ SiO_2He transitioning from a solid to a superionic phase. At 800 GPa, $Pnma$ SiO_2He remains solid up to 8000 K, and heating to 9000 K transforms it to a superionic phase with partial He diffusion (Figure S6(b) [55]) with a diffusion

coefficient of $D^{\text{He}} = 1.31 \times 10^{-6} \text{ cm}^2\text{s}^{-1}$. Further heating to 10,000 K increases the diffusion of He; its coefficients becomes $D^{\text{He}} = 3.43 \times 10^{-6} \text{ cm}^2\text{s}^{-1}$. At 12,000 K, all atoms are diffusive (see Fig. S6(d)), with higher diffusion coefficients of $D^{\text{Si}} = 8.91 \times 10^{-5} \text{ cm}^2\text{s}^{-1}$, $D^{\text{O}} = 1.07 \times 10^{-4} \text{ cm}^2\text{s}^{-1}$, and $D^{\text{He}} = 1.44 \times 10^{-4} \text{ cm}^2\text{s}^{-1}$. Previous studies show that with the increasing temperature, the H atoms in CH_4 -He [31] and H_2O -He [26–28] systems become diffusive firstly and transform into superionic phase, while the He atoms are easier to diffuse in NH_3 -He [28–30]. As compared to these He-incorporation compounds, the critical temperatures transition from a solid to a superionic or fluid phase for SiO_2He are higher than them, displaying the He atoms diffusing firstly, which is mainly caused by the following two reasons. First, the atomic mass of He atom is larger than that of H atom. Second, the HeO_7 polyhedron configuration in the SiO_2He unit cell makes the He atoms be trapped inside the cage, which restricts its diffusion. Figure S7 shows the estimated pressure-temperature conditions for the solid, superionic, and fluid phases of SiO_2He and reveals that the incorporation of He notably inhibits the melting of silica.

In conclusion, combining first-principles theory and structural prediction, we report a $Pnma$ SiO_2He phase that is stable under planetary interior conditions. This phase is stable over a large pressure range from 607 GPa to at least 1 TPa at 0 K. It is composed of four equivalent seven-coordinated SiO_7 polyhedra, which have not been found previously in the ground state of silica. AIMD calculations show the possibility of solid SiO_2He being present at the CMBs of the gas planets of our solar system as well as in super-Earths more massive than $5.7 M_\oplus$. The present results not only benefit our understanding of the high-pressure behavior of materials, but can also broaden the family of He-containing compounds and provide assistance in understanding the structural models and evolution of giant planets' interiors.

The authors acknowledge funding from the NSFC under grants No. 12074154, No. 11804129, No. 11722433 and No. 11804128, and the funding from the Science and Technology Project of Xuzhou under grant No. KC19010. Y.L. acknowledges the funding from the Six Talent Peaks Project and 333 High-level Talents Project of Jiangsu Province. S.D. acknowledges the founding from Postgraduate Research & Practice Innovation Program of Jiangsu Province No. KYCX20_2223. All the calculations were performed at the High Performance Computing Center of the School of Physics and Electronic Engineering of Jiangsu Normal University.

- [1] K. Umemoto, R. M. Wentzcovitch, and P. B. Allen, *Science* **311**, 983 (2006).
- [2] T. Tsuchiya and J. Tsuchiya, *Proc. Natl. Acad. Sci.* **108**, 1252 (2011).
- [3] M. Millot, N. Dubrovinskaya, A. Černok, S. Blaha, L. Dubrovinsky, D. G. Braun, P. M. Celliers, G. W. Collins, J. H. Eggert, and R. Jeanloz, *Science* **347**, 418 (2015).

- [4] L. Levien, C. T. Prewitt, and D. J. Weidner, *Am. Mineral.* **65**, 920 (1980).
- [5] L. Levien and C. T. Prewitt, *Am. Mineral.* **66**, 324 (1981).
- [6] N. L. Ross, J. Shu, and R. M. Hazen, *Am. Mineral.* **75**, 739 (1990).
- [7] M. Akaogi and A. Navrotsky, *Phys. Earth Planet. Inter.* **36**, 124 (1984).
- [8] K. J. Kingma, R. E. Cohen, R. J. Hemley, and H.-k. Mao, *Nature* **374**, 243 (1995).
- [9] K. Driver, R. Cohen, Z. Wu, B. Militzer, P. L. Ríos, M. Towler, R. Needs, and J. Wilkins, *Proc. Natl. Acad. Sci.* **107**, 9519 (2010).
- [10] L. Dubrovinsky, N. Dubrovinskaia, S. Saxena, F. Tutti, S. Rekhi, T. Le Bihan, G. Shen, and J. Hu, *Chem. Phys. Lett.* **333**, 264 (2001).
- [11] A. R. Oganov, M. J. Gillan, and G. D. Price, *Phys. Rev. B* **71**, 064104 (2005).
- [12] Y. Kuwayama, K. Hirose, N. Sata, and Y. Ohishi, *Science* **309**, 923 (2005).
- [13] Y. Kono, Y. Shu, C. Kenney-Benson, Y. Wang, and G. Shen, *Phys. Rev. Lett.* **125**, 205701 (2020).
- [14] C. Liu, J. Shi, H. Gao, J. Wang, Y. Han, X. Lu, H.-T. Wang, D. Xing, and J. Sun, *Phys. Rev. Lett.* **126**, 035701 (2021).
- [15] S. Wu, K. Umemoto, M. Ji, C.-Z. Wang, K.-M. Ho, and R. M. Wentzcovitch, *Phys. Rev. B* **83**, 184102 (2011).
- [16] M. J. Lyle, C. J. Pickard, and R. J. Needs, *Proc. Natl. Acad. Sci.* **112**, 6898 (2015).
- [17] T. Duffy, N. Madhusudhan, and K. Lee, *Treatise on Geophysics* **2** (2015).
- [18] R. Scipioni, L. Stixrude, and M. P. Desjarlais, *Proc. Natl. Acad. Sci.* **114**, 9009 (2017).
- [19] F. González-Cataldo, S. Davis, and G. Gutiérrez, *Sci. Rep.* **6**, 1 (2016).
- [20] H. Niu, A. R. Oganov, X.-Q. Chen, and D. Li, *Sci. Rep.* **5**, 1 (2015).
- [21] T. Guillot, *Phys. Today* **57**, 63 (2004).
- [22] D. J. Stevenson, *Proc. Natl. Acad. Sci.* **105**, 11035 (2008).
- [23] M. Jackson, J. Konter, and T. Becker, *Nature* **542**, 340 (2017).
- [24] J. Zhang, J. Lv, H. Li, X. Feng, C. Lu, S. A. Redfern, H. Liu, C. Chen, and Y. Ma, *Phys. Rev. Lett.* **121**, 255703 (2018).
- [25] N. Nettelmann, K. Wang, J. J. Fortney, S. Hamel, S. Yellamilli, M. Bethkenhagen, and R. Redmer, *Icarus* **275**, 107 (2016).
- [26] C. Liu, H. Gao, Y. Wang, R. J. Needs, C. J. Pickard, J. Sun, H.-T. Wang, and D. Xing, *Nat. Phys.* **15**, 1065 (2019).
- [27] H. Liu, Y. Yao, and D. D. Klug, *Phys. Rev. B* **91**, 014102 (2015).
- [28] Y. Bai, Z. Liu, J. Botana, D. Yan, H.-Q. Lin, J. Sun, C. J. Pickard, R. J. Needs, and M.-S. Miao, *Commun. Chem.* **2**, 1 (2019).
- [29] J. Shi, W. Cui, J. Hao, M. Xu, X. Wang, and Y. Li, *Nat. Commun.* **11**, 1 (2020).
- [30] C. Liu, H. Gao, A. Hermann, Y. Wang, M. Miao, C. J. Pickard, R. J. Needs, H.-T. Wang, D. Xing, and J. Sun, *Phys. Rev. X* **10**, 021007 (2020).
- [31] H. Gao, C. Liu, A. Hermann, R. J. Needs, C. J. Pickard, H.-T. Wang, D. Xing, and J. Sun, *Natl. Sci. Rev.* **7**, 1540 (2020).
- [32] B. Monserrat, M. Martinez-Canales, R. J. Needs, and C. J. Pickard, *Phys. Rev. Lett.* **121**, 015301 (2018).
- [33] H. Gao, J. Sun, C. J. Pickard, and R. J. Needs, *Phys. Rev. Mater.* **3**, 015002 (2019).
- [34] Y. Li, X. Feng, H. Liu, J. Hao, S. A. Redfern, W. Lei, D. Liu, and Y. Ma, *Nat. Commun.* **9**, 1 (2018).
- [35] X. Dong, A. R. Oganov, A. F. Goncharov, E. Stavrou, S. Lobanov, G. Saleh, G.-R. Qian, Q. Zhu, C. Gatti, V. L. Deringer, *et al.*, *Nat. Chem.* **9**, 440 (2017).
- [36] Z. Liu, J. Botana, A. Hermann, S. Valdez, E. Zurek, D. Yan, H.-q. Lin, and M.-s. Miao, *Nat. Commun.* **9**, 1 (2018).
- [37] Y. Wang, J. Zhang, H. Liu, and G. Yang, *Chem. Phys. Lett.* **640**, 115 (2015).
- [38] T. Sato, H. Takada, T. Yagi, H. Gotou, T. Okada, D. Wakabayashi, and N. Funamori, *Phys. Chem. Miner.* **40**, 3 (2013).
- [39] M. Matsui, T. Sato, and N. Funamori, *Am. Mineral.* **99**, 184 (2014).
- [40] Y. Wang, J. Lv, L. Zhu, and Y. Ma, *Phys. Rev. B* **82**, 094116 (2010).
- [41] Y. Wang, J. Lv, L. Zhu, and Y. Ma, *Comput. Phys. Commun.* **183**, 2063 (2012).
- [42] Y. Li, J. Hao, H. Liu, Y. Li, and Y. Ma, *J. Chem. Phys.* **140**, 174712 (2014).
- [43] Y. Li, J. Hao, H. Liu, S. Lu, and S. T. John, *Phys. Rev. Lett.* **115**, 105502 (2015).
- [44] Y. Li, L. Wang, H. Liu, Y. Zhang, J. Hao, C. J. Pickard, J. R. Nelson, R. J. Needs, W. Li, Y. Huang, *et al.*, *Phys. Rev. B* **93**, 020103 (2016).
- [45] W. Cui and Y. Li, *Chin. Phys. B* **28**, 107104 (2019).
- [46] G. Kresse and J. Furthmüller, *Phys. Rev. B* **54**, 11169 (1996).
- [47] G. Kresse and J. Furthmüller, *Comput. Mater. Sci.* **6**, 15 (1996).
- [48] J. P. Perdew, J. A. Chevary, S. H. Vosko, K. A. Jackson, M. R. Pederson, D. J. Singh, and C. Fiolhais, *Phys. Rev. B* **46**, 6671 (1992).
- [49] J. P. Perdew, K. Burke, and M. Ernzerhof, *Phys. Rev. Lett.* **77**, 3865 (1996).
- [50] G. Kresse and D. Joubert, *Phys. Rev. B* **59**, 1758 (1999).
- [51] A. Togo, F. Oba, and I. Tanaka, *Phys. Rev. B* **78**, 134106 (2008).
- [52] S. Nosé, *J. Chem. Phys.* **81**, 511 (1984).
- [53] W. G. Hoover, *Phys. Rev. A* **31**, 1695 (1985).
- [54] K. Momma and F. Izumi, *J. Appl. Crystallogr.* **44**, 1272 (2011).
- [55] See Supplemental Material at [URL will be inserted by publisher]. It contains Structural parameters, Polyhedron Structures, Phonon dispersions, Bandgap at different pressures, MSD and atomic trajectories, Discovered Super-Earths.
- [56] G. Henkelman, A. Arnaldsson, and H. Jónsson, *Comput. Mater. Sci.* **36**, 354 (2006).
- [57] T. Guillot, *Science* **286**, 72 (1999).
- [58] F. Wagner, N. Tosi, F. Sohl, H. Rauer, and T. Spohn, *Astron. Astrophys.* **541**, A103 (2012).
- [59] R. Helled, N. Nettelmann, and T. Guillot, *Space Sci. Rev.* **216**, 1 (2020).